Tannic Acid Accelerates Cutaneous Wound Healing in Rats Via Activation of the *ERK 1/2* Signaling Pathways

Yaqin Chen,[1,†] Lvbo Tian,[2,†] Fengyu Yang, [1,†] Wenzhi Tong,[1] Renyong Jia,[1] Yuanfeng Zou,[1] Lizi Yin,[1] Lixia Li,[1] Changliang He,[1] Xiaoxia Liang,[1] Gang Ye,[1] Cheng Lv,[1] Xu Song,[1,*] and Zhongqiong Yin[1,*]

[1]*Natural Medicine Research Center, College of Veterinary Medicine, Sichuan Agricultural University, Chengdu, China.*
[2]*Sichuan International Travel Health Care Center, Chengdu, China.*
[†]*Cofirst authors.*

Objective: This study was aimed to evaluate the effect of tannic acid (TA), a natural plant polyphenol astringent, on wound healing *in vitro* and *in vivo*, and to elucidate the underlying molecular signaling pathway in the wound healing.

Approach: Cutaneous skin wounds were created in rats and then treated until closure with purified TA, serum or tissue samples were collected to test the concentration of factors by enzyme-linked immunosorbent assay (ELISA), and the expression in gene or protein was measured by quantitative real-time polymerase chain reaction or Western blot. We explored the cell-/dose-specific responses of TA (0.1–0.4 μg/mL) on proliferation and gene and protein expression of fibroblast NIH 3T3 cells.

Results: The wounds on rats treated by TA got healed faster than those in the untreated group. The histopathology study showed that TA accelerated re-epithelialization and increase in hair follicles could be detected. The levels of growth factors including basic fibroblast growth factor (bFGF), transforming growth factor-beta, and vascular endothelial growth factor in TA-treated groups were all increased, and the content of interleukin-1 (IL-1) and IL-6 was decreased significantly when compared with that of the untreated group. The NIH 3T3 cells grow faster in 6 h at concentration of 0.1 μg/mL, and the expression of bFGF in gene and protein was increased significantly in the 0.1 μg/mL TA group. Further study revealed that the protein levels of bFGF, extracellular signal regulated kinase (Erk) 1/2, and P-Erk 1/2 in Erk 1/2 pathway were increased after TA treatment.

Innovation: The role of TA in wound healing efficacy is unclear; this study, therefore, assesses the effects of TA on wound healing in different periods and the underlying molecular mechanisms.

Conclusion: These results suggested that TA could accelerate wound healing through modulation of inflammatory cytokines and growth factors and activate Erk 1/2 pathway. In conclusion, TA may be a potential agent in promoting wound healing.

Keywords: wound healing, tannic acid, rats, growth factors, pathway

Zhongqiong Yin, PhD

Submitted for publication September 11, 2018. Accepted in revised form February 23, 2019.

*Correspondence: Natural Medicine Research Center, College of Veterinary Medicine, Sichuan Agricultural University, Chengdu 611130, China (e-mail: yinzhongq@163.com).

Xu Song, PhD

*Correspondence: Natural Medicine Research Center, College of Veterinary Medicine, Sichuan Agricultural University, Chengdu 611130, China (e-mail: songx@sicau.edu.cn).

DOI: 10.1089/wound.2018.0853

INTRODUCTION

Compared with other tissues, skin is the most frequently injured tissue. Wound healing is a dynamic and complex multistep process to repair and restructure, which involves the regulated integration of complex biological events including cell migration, proliferation, and extracellular matrix remodeling.[1–3] The wound healing process is divided into sequential, yet overlapping phases: hemostasis, inflammation, proliferation, and remodeling.[4,5] Tremendous progress has been made in recent years to identify the key cellular and molecular events responsible for wound healing.[2,4,6,7] Upon injury to the skin, the epidermal barrier is disrupted, and interleukin-1 (IL-1) is the first factor released by keratinocytes.[3] Then clotting cascade is activated in the wound site that induces hemostasis and provides a matrix for the influx of inflammatory cells. Macrophages initiate the development of granulation tissue and release a variety of proinflammatory cytokines (IL-1 and IL-6) and growth factors (fibroblast growth factor [FGF], transforming growth factor-beta [TGF-β], and platelet-derived growth factor [PDGF]). With the assistance of platelet-released vascular endothelial growth factor (VEGF) and FGF, endothelial cells proliferate and angiogenesis ensues.[1–3,7]

In recent years, many research studies have indicated the potential in exploring drug extracts from plants for promoting wound healing.[1] For examples, *Mimosa pudica* that is found to be rich in tannins, and the total tannin content was reported to exhibit good wound healing activity; lucidone accelerates wound healing through the cooperation of keratinocyte/fibroblast/endothelial cell growth and migration and macrophage inflammation through PI3K/AKT, Wnt/β-catenin, and NF-κB signaling cascade activation[2]; and tazarotene promotes neovascularization and tissue repair through its action on retinoic acid signaling.[6] These are potentially useful in promoting the healing of wounds, skin inflammation, and burns. Tannic acid (TA) is a plant polyphenol found abundantly in the galls of *Rhus* and *Quercus* species, and it is categorized as antioxidant, antimicrobial, antiviral, and anti-inflammatory agents.[8–10] Structurally, TA has glucose moiety as core, and hydroxyl groups of glucose are esterified with five digallic acid (Fig. 1). In the early 20th century, it

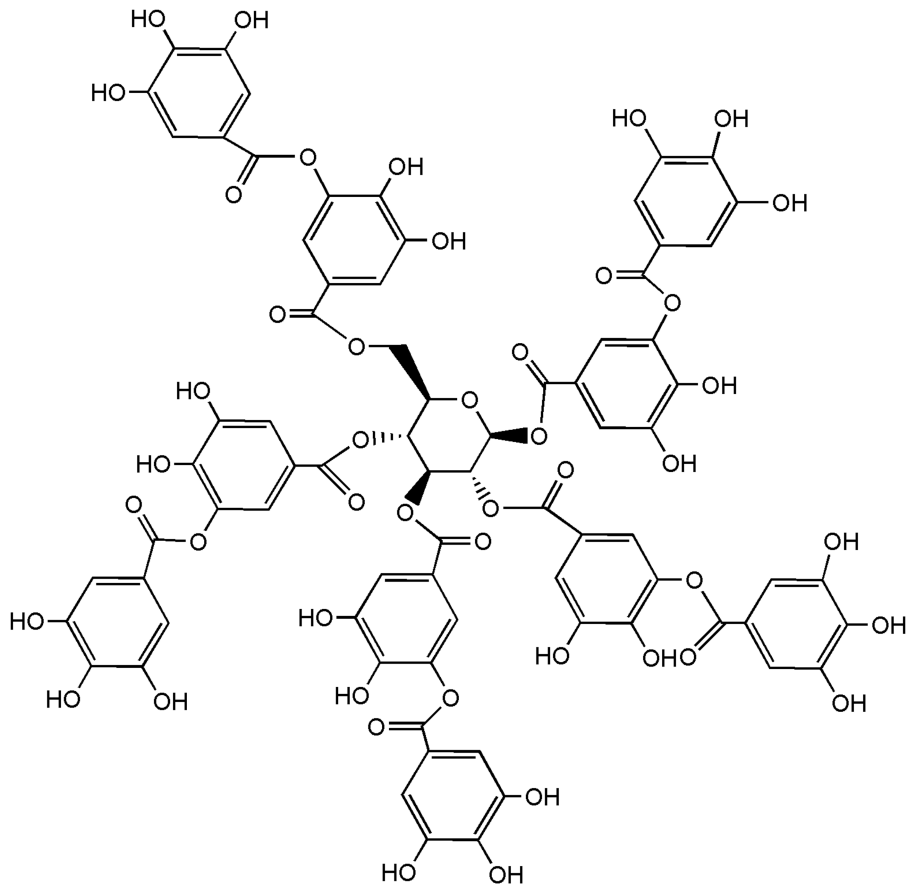

Figure 1. The structure of TA. TA, tannic acid.

was used in the treatment of burns and later it was discontinued because of its inconclusive necrotic effect on liver. Recent toxicity studies on highly purified TA in clinical trials confirmed that the toxic effects observed in patients with burn were mainly due to contaminants (particularly gallic acid) present in the preparations.[8,10,11]

Since the plant extract containing TA exhibited wound healing efficacy, this study is, therefore, an attempt to assess the effects of TA on wound healing and the underlying molecular mechanisms *in vivo* and *in vitro*.

CLINICAL PROBLEM ADDRESSED

It was reported that there were >1.25 million people suffering from burns and 6.5 million people having chronic skin ulcers caused by pressure, venous stasis, or diabetes mellitus in the world.[4,5] Although many medicines showed a good activity on wound healing, they also caused the formation of scar. Our study aimed to prove that TA could ameliorate scar formation and promote hair follicle regeneration. The findings from this study indicated that TA could stimulate hair follicle regeneration and the growth of fibroblast NIH 3T3 cells, accelerate wound healing through modulation of inflammatory cytokines and growth factors, and activation of extracellular signal regulated kinase (Erk) 1/2 pathway. TA may be a potential agent in promoting wound healing

MATERIALS AND METHODS

Preparation of TA

TA was purchased from Solarbio Corp. (Cas 1401-55-4, HPLC ≥98%, China). Stock solutions of 2 g/mL TA were prepared using sterile water and stored at –20°C. All solutions were freshly prepared from stock solutions before each experiment and kept away from light exposure.

Animal model and treatment

All animal experiments were conducted after getting prior permission from Institutional Animal Ethics Committee that followed the instructions prescribed by the committee for the purpose of control and supervision of experiments on animals.

Seventy-two healthy male Sprague Dawley rats, weighing 200–220 g, were provided by the Chengdu Dossy Experimental Animals Co., Ltd. (License No. SCXK [chuan] 2015-030). They were kept in well-ventilated sterile polypropylene cages in the animal houses of Sichuan Agricultural University (Chengdu, China). Based on the guidelines of the international committee on laboratory animals, they were housed in a standard environmental condition (25°C ± 3°C, 55% ± 5% humidity, 12 h light/dark cycle) and fed with rodent standard diets and water *ad libitum*. Experiments were started after acclimating the animals for 1 week.

The rats were anesthetized by intraperitoneal injection of 10% chloral hydrate (0.3 mL/100 g), followed by fixing in a prone position. After back hair removal and alcohol disinfection, epidermis was peeled off at the same site near the neck with sterile dermal biopsy punches to form two circular wounds of 0.8 cm in diameter and depth reaching the superficial layer of deep fascia. Square gauze larger than the size of wounds was used to cover the wounds.

Sixty rats with wounds were randomly divided into five groups: group B (model group), group C (Yunnan Baiyao [YB] group), group D [1.5 g/mL TA (h) group], group E [1.0 g/mL TA (m) group], and group F [0.5 g/mL TA (l) group]. Normal rats were also used as blank control (group A). They were fed in separate cages. In group B, 0.25 mL of normal saline was applied on the wounds. In group C, 0.25 mL of 0.5 g/mL YB dissolved in normal saline was applied. In group D, group E, and group F, 0.25 mL TA at different concentrations of 1.5, 1.0, and 0.5 g/mL, respectively, was used. The treatment was conducted once a day. On the 3rd, 10th, and 21st day after treatment, four rats were sacrificed in each group under anesthesia, and the skin tissue was collected for later experiments.

Wound healing percentage assay

Each wound site was digitally photographed everyday at the indicated time intervals, and wound areas were determined on photographs using Adobe Photoshop (version 7.0; Adobe Systems, San Jose, CA). Changes in wound areas over time were expressed as the percentage of the initial wound areas.

Histopathology assay

Tissues from wound sites were embedded in paraffin and cut into 4-mm sections. The sections were deparaffinized in three changes of xylene and rehydrated through a graded ethanol series. The sections were stained with hematoxylin for 5 min and with eosin for 1 min in hematoxylin–eosin staining. Masson staining was performed to identify the extracellular matrix (collagen fiber). The sections were stained according to the instructions from modified Masson's Trichrome Stain Kit (Solarbio, Beijing, China). All the stained slides were visualized using a bright-field optical microscope (Nikon TE-200U).

Cytokines assay

The blood samples used for cytokine examination were collected into nonpreservative tubes. The

serum was separated by centrifugation at 3,000 g for 10 min after coagulation. The concentrations of IL-1, IL-6, basic FGF (bFGF), VEGF, hepatocyte growth factor (HGF), and fibronectin (FN) in the serum were measured followed by the guidance of R&D rats enzyme-linked immunosorbent assay (ELISA) kits.

Real-time polymerase chain reaction assay

To reveal the molecular cascades, the determination of related mRNA levels was necessary. In brief, total RNA from skin was extracted by Total RNA Kit (No. R6934-01; OMEGA) according to manufacturer's protocol. Then, RNA quality was determined by measuring the OD260/OD280 ratio (>2.0). RNA (1 μg) of each tissue was reverse transcribed by PrimeScript™ RT Reagent Kit with gDNA Eraser (No. RR047A; Takara Bio, Otsu, Japan). cDNA (1 μL) of each tissue's sample was used for real-time polymerase chain reaction (RT-PCR) with SYBR Green Supermix Kit (No. 1708882; Bio-Rad, Hercules, CA) in a Bio-Rad CFX Connect™ Real-Time PCR System (Bio-Rad). The following primers for rat samples were used: TGF-β, forward (F)-5′CTGCTGACCCCCACTGATAC3′ and reverse (R)-5′AGCCCTGTATTCCGTCTCCT3′; VEGF, F-5′CGAGGAAAGGGAAAGGGTCA3′ and R-5′TTC TCCGCTCTGAACAAGGC3′; HGF, F-5′ACAGCTT TTTGCCTTCGAGC3′ and R-5′GCTTGTGAAACA CCAGGGTC3′; bFGF, F-5′TTTGGCTAGTTTGCT GGGAAG3′ and R-5′TAAAGCTGAGCCCAAATC GC3′; IL-1, F-5′CTGTGCATCTTCGACAGGGA3′ and R-5′AGCACGTAGTTGGGGCTTAG3′; IL-6, F-5′CCTACCCCAACTTCCAATGCT3′ and R-5′GGT CTTGGTCCTTAGCCACT3′; FN, F-5′CCCTTCCA CACCCCAATCTT3′ and R-5′CTGGGTTGTTGGT GGGATGT3′; and β-actin, F-5′GGAGATTACTGC CCTGGCTCCTAGC3′ and R-5′GGCCGGACTCA TCGTACTCCTGCTT3′. The PCR conditions were initial denaturation at 95°C for 3 min, followed by 40 cycles of denaturation at 95°C for 30 s, annealing for 30 s at 51–61°C, and extension at 72°C for 30 s. A melting curve of PCR products (65–95°C) was also performed to ensure the absence of artifacts. The relative quantification of tested gene expression was calculated using the $2^{-\Delta\Delta Ct}$ method. Sequences for primers were designed by Oligo 7 software. Primers were synthesized by Liuhe Genomics Technology Co., Ltd. (Beijing, China).

Western blotting assay

To clearly illuminate whether a signaling pathway was activated, the total protein was extracted for evaluation. The skins were collected and washed with cold phosphate-buffered saline, and then were lysed with lysis buffer containing 1 mM inhibitor PMSF (No. AR1178; Boster). The total protein of skin was extracted by the mammalian tissue extracted kit (No. AR0101-30; Boster). The concentrations of protein were determined by the BCA protein assay kit (No. AR0146; Boster). Then, each sample was subsequently denatured with 4× dual color protein loading buffer at 100°C for 5 min (No. AR1142; Boster). Equivalent amounts of protein (30 μg) from each sample were separated by sodium dodecyl sulfate polyacrylamide gel electrophoresis and subsequently transferred to polyvinylidene fluoride membranes (Millipore). Protein blots were blocked with 5% skim milk or 5% bovine serum albumin at room temperature for 1 h and then were incubated with primary antibodies against bFGF (Abcam), ERK 1/2 (CST), and P-ERK 1/2 (CST) overnight at 4°C. After washing three times with TBST (20 mM Tris–HCl [pH 7.4], 100 mM NaCl and 0.1% [w/v] Tween 20) buffer and then protein blots were exposed to the relative peroxidase-conjugated secondary antibody (goat antimouse or goat antirabbit; CST) for 1 h at room temperature. Immunoreactive bands were visualized with chemiluminescence (ECL prime; Pierce Chemical) using standard X-ray film (Kodak X-Omat AR) and quantified relative to β-actin (CST) using National Institutes of Health Image J software.

Cell culture

NIH 3T3 fibroblasts were cultured in Dulbecco's modified Eagle's medium supplemented with 10% new born calf serum at 37°C in 5% CO_2 atmosphere. The cells were harvested by trypsin–ethylenediaminetetraacetic acid treatment and used for seeding. The scaffold was then placed in 96-well polystyrene plates and seeded with 5×10^4 cells per well. The culture medium was changed every 2 days. Cell proliferation was monitored at 6, 12, and 24 h using Cell Counting Kit-8. The cells or the supernatant were collected for monitoring the gene expression or protein expression of growth factors.

Statistical analysis

The data are presented as the mean ± standard deviation, and all of the statistical analyses were performed using SPSS 17.0 statistical software. For histograms used in cytokine examination, mRNA levels expression and protein's mean density expression were plotted by GraphPad Prism 6 software. Statistical significance of the data from the control and experimental groups was compared by one-way analysis of variance and the least significant difference test. $p < 0.05$ was considered statistically significant.

Table 1. *Effect of TA on wound healing (n = 4, %)*

Days	*Model*	*YB*	*TA (h)*	*TA (m)*	*TA (l)*
0th	0.00 ± 0.00	0.00 ± 0.00	0.00 ± 0.00	0.00 ± 0.00	0.00 ± 0.00
3rd	17.90 ± 8.06^{bcde}	47.95 ± 4.17^{a}	46.13 ± 17.96^{a}	37.73 ± 3.45^{a}	36.16 ± 7.63^{a}
5th	27.38 ± 7.55^{bcde}	56.56 ± 10.39^{a}	58.30 ± 13.98^{a}	51.60 ± 7.36^{a}	46.86 ± 4.07^{a}
7th	43.83 ± 14.95^{bc}	72.71 ± 4.91^{a}	64.57 ± 12.40^{a}	56.73 ± 5.10^{b}	55.07 ± 2.61^{b}
9th	55.90 ± 11.97^{bc}	82.84 ± 5.77^{a}	73.37 ± 10.48^{a}	64.59 ± 4.89^{b}	67.85 ± 9.11^{b}
11th	72.82 ± 10.16^{be}	89.77 ± 1.88^{a}	80.96 ± 5.49	80.79 ± 8.03	87.48 ± 11.61^{a}
13th	84.51 ± 2.24	93.52 ± 6.89^{a}	89.97 ± 2.92^{a}	95.11 ± 4.52^{a}	93.59 ± 6.10^{a}
15th	97.72 ± 1.96	99.02 ± 1.16	97.98 ± 1.02	98.83 ± 1.74	98.45 ± 2.42
17th	98.43 ± 1.97	100.00 ± 0.00	99.00 ± 1.90	100.00 ± 0.00	100.00 ± 0.00

Model, model group; YB, Yunnan Baiyao group; TA (h), high-dose group; TA (m), middle-dose group; TA (l), low-dose group.
The superscript letters "a, b, c, d, and e," respectively, means significantly different with "model, YB, TA (h), TA (m), and /TA (l)" group.
TA, tannic acid.

RESULTS

Wound healing percentage assay

As shown in Table 1, TA treatment accelerated the wound closure, and the wound gradually disappeared, which was faster than the control (Fig. 2). The wound sizes in the YB- and TA-treated rats decreased quickly, the significant decrease in the wound size after TA/YB application (within 5 days of postwounding) amplified the potent cutaneous wound healing capability of TA, and at the 5th day the wound size almost changed 50% when compared with the model group. At the 17th day, the wound got healed in the pretreated rats, although the healing rate of the model group was 98.43%; comparing the TA-treated rats with YB-treated rats, the wound sizes decreased faster in the YB-group after day 7 and almost got healed at the 15th day.

Histopathology assay

Images from histopathological studies further indicated that TA application accelerated re-epithelialization and closed the wound margins, whereas the wound margins remained open in the untreated group. On day 3, the structure of hair follicle, sebaceous gland, and subcutaneous tissue in the blank control group were normal; in other groups, the injuries led to a certain degree of tissue defect, neutrophils gathered toward the wounds, and exudation of large number of red cells had appeared (Fig. 3-1). On day 10, neutrophils and red cells were observed only in the untreated group. The structure of keratoderma, stratum granulosum, stratum spinosum, and basal layer was normal and more granulation tissue grew and local tissue was repaired well in treated groups. More hair follicle grew in the YB-treated and middle dose of TA-treated groups (Fig. 3-2). On day 21, although the rats in each group had normal and complete tissue, TA treatment group accelerated re-epithelialization and grew more hair follicle than the model group, which was similar with the YB-treated rats (Fig. 3-3). By contrast, the TA-treated animals had a thin and well-organized epidermis with well-formed hair follicles and much better organized collagen (Fig. 4). We found that TA could stimulate hair follicle neogenesis and reduce scarring in rats.

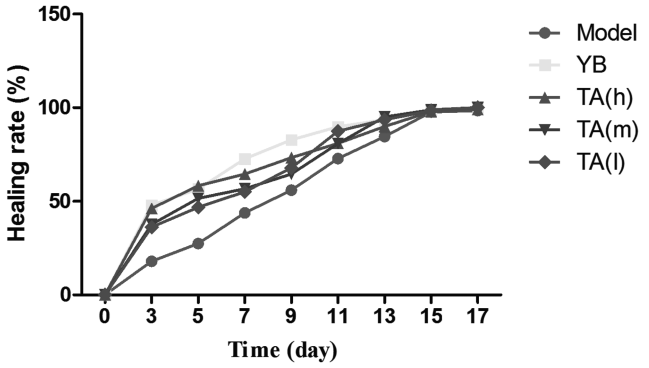

Figure 2. Effect of TA on wound healing rate.

Cytokine assay

Upon injury to the skin, the epidermal barrier is disrupted and keratinocytes release proinflammatory cytokines, particularly IL-1 and IL-6. The results of proinflammatory cytokine concentrations in serum are shown in Fig. 5. Compared with blank control group, the productions of IL-1 were significantly increased in the model group on day 3 ($p < 0.05$). On the contrary, these proinflammatory cytokines in YB and high dose of TA groups were significantly decreased ($p < 0.05$) when compared with the model group. IL-6 was relatively increased ($p > 0.05$) on day 3 and significantly decreased on day 10, especially in low dose of TA-treated group ($p < 0.05$). On day 21, the levels of IL-1 and IL-6 in all groups were recovered to normal.

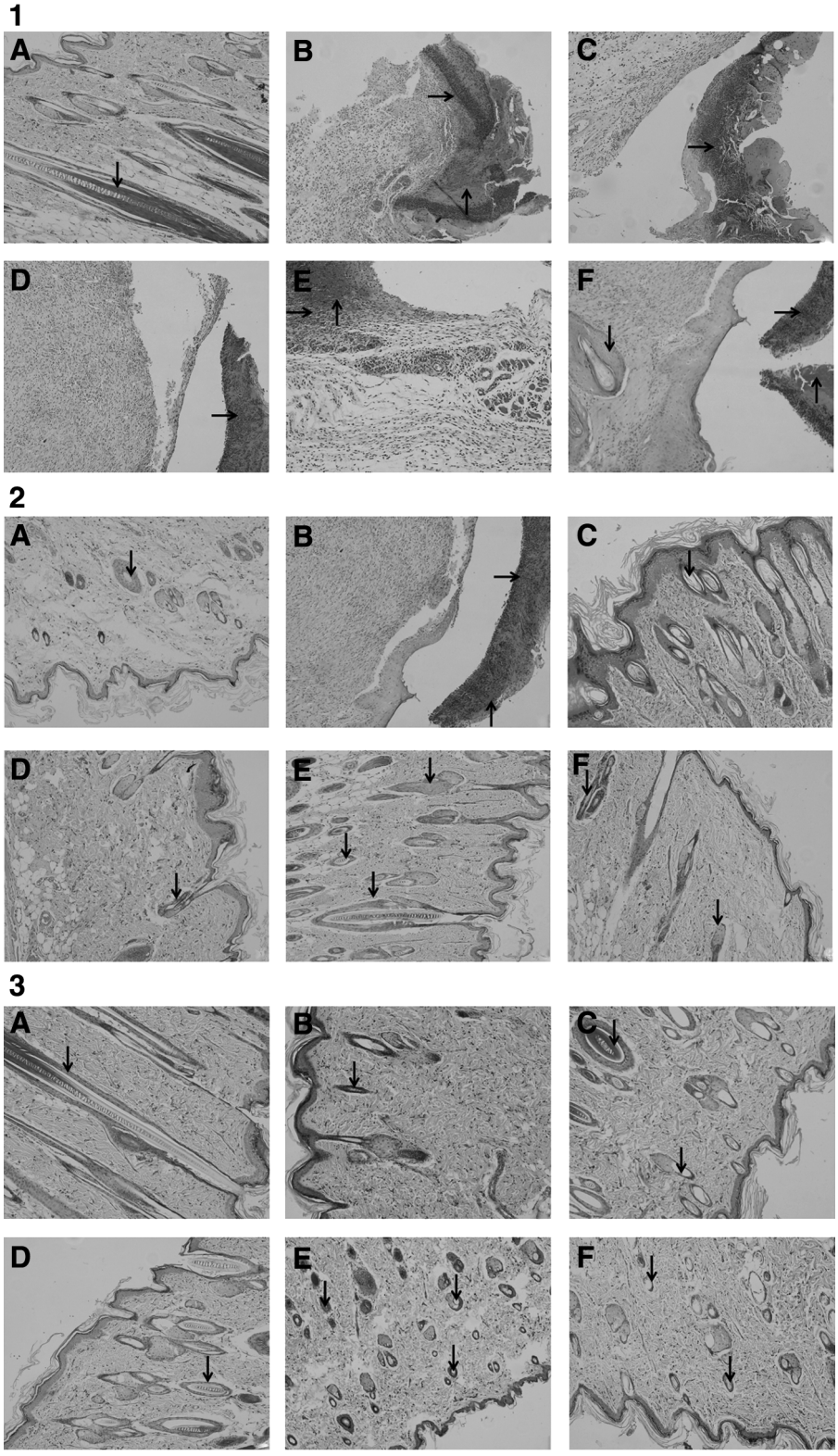

Figure 3. **(1)** A histological examination of skin in the wound area on day 3 (HE, 100×). **(A)** Blank control group, **(B)** model group, **(C)** YB group, **(D)** high-dose group, **(E)** middle-dose group, **(F)** low-dose group; hair follicle (↓); red blood cell (↑); neutrophile granulocyte (→). **(2)** A histological examination of skin in the wound area on day 10 (HE, 100×). **(A)** Blank control group, **(B)** model group, **(C)** YB group, **(D)** high-dose group, **(E)** middle-dose group, **(F)** low-dose group; hair follicle (↓); red blood cell (↑); neutrophile granulocyte (→). **(3)** A histological examination of skin in the wound area on day 21 (HE, 100×). **(A)** Blank control group, **(B)** model group, **(C)** YB group, **(D)** high-dose group, **(E)** middle-dose group, **(F)** low-dose group; hair follicle (↓). HE, hematoxylin–eosin; YB, Yunnan Baiyao.

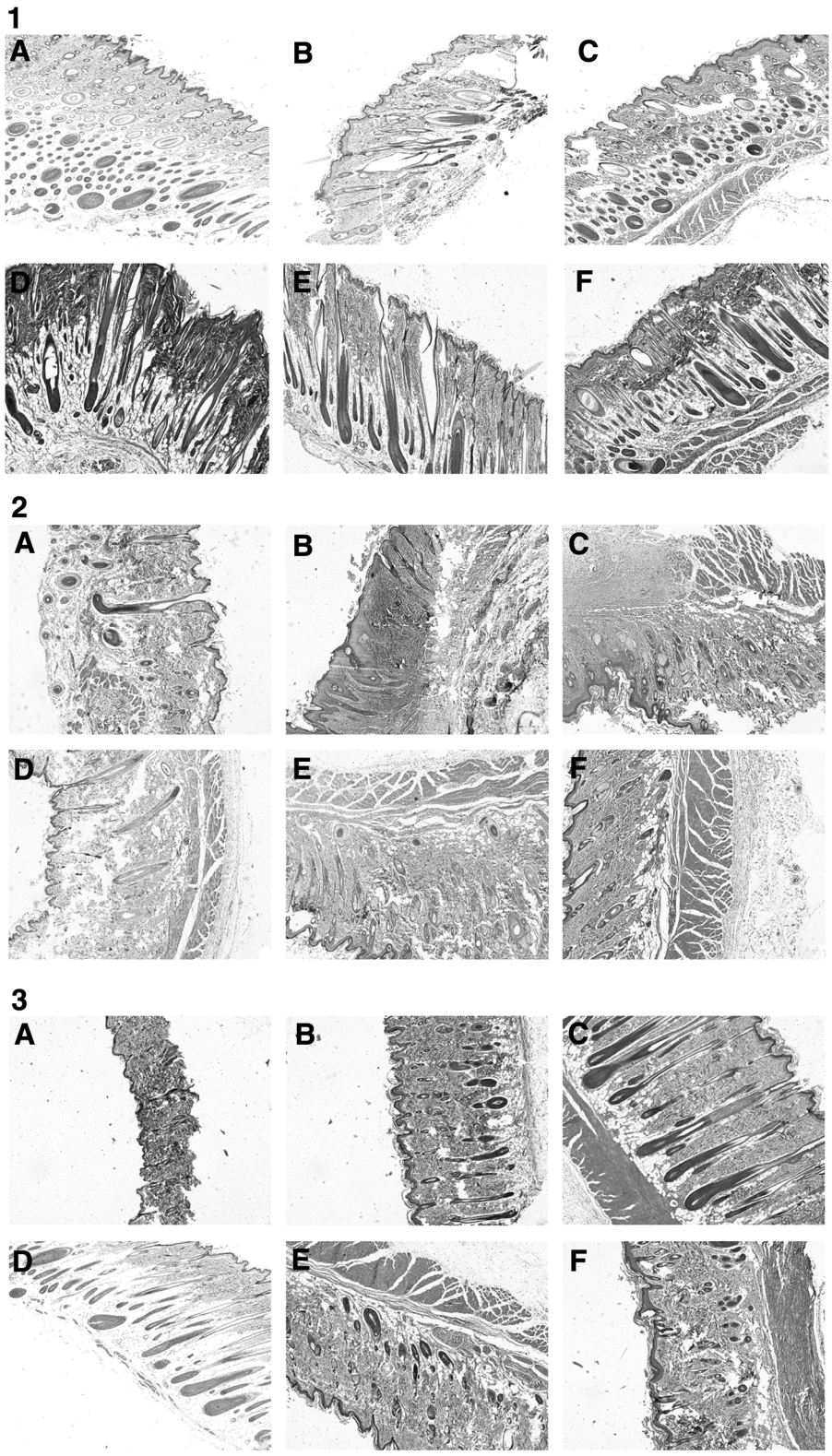

Figure 4. **(1)** A histological examination of skin in the wound area on day 3 (Masson, 40×). **(A)** Blank control group, **(B)** model group, **(C)** YB group, **(D)** high-dose group, **(E)** middle-dose group, **(F)** low-dose group. **(2)** A histological examination of skin in the wound area on day 10 (Masson, 40×). **(A)** Blank control group, **(B)** model group, **(C)** YB group, **(D)** high-dose group, **(E)** middle-dose group, **(F)** low-dose group. **(3)** A histological examination of skin in the wound area on day 21 (Masson, 40×). **(A)** Blank control group, **(B)** model group, **(C)** YB group, **(D)** high-dose group, **(E)** middle-dose group, **(F)** low-dose group.

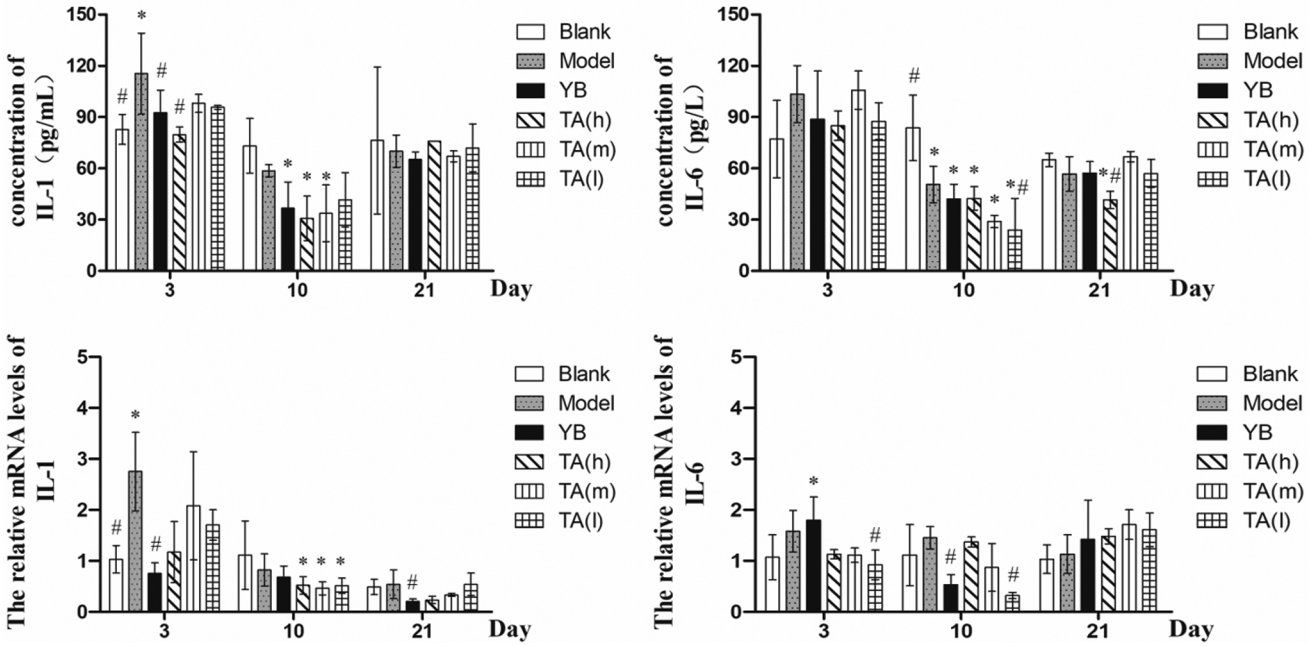

Figure 5. The effects of TA on the content of inflammatory cytokines were detected by ELISA or RT-PCR. Blank and model represent the groups that were treated as blank control or model group, and YB, TA (h), TA (m), and TA (l) represent the groups that were pretreated with YB, high, middle, and low dose of TA. The values are presented as means ± standard deviation (10 rats/group).* $p < 0.05$ versus blank control group; # $p < 0.05$ versus model group. ELISA, enzyme-linked immunosorbent assay; RT-PCR, real-time polymerase chain reaction.

Blood components are released into the wound site when the body was injured, and then platelets degranulated to release alpha granules, which secrete growth factors, such as bFGF, VEGF, TGF-β, HGF, and FN. Fig. 6 shows the concentrations of these growth factors in serum. Compared with those of the blank control group and the model group, the concentrations of these growth factors did not show significant differences in the treated groups on day 3, except the treatments had significantly lower levels of HGF relative to the blank control; the expression levels of bFGF, TGF-β, and FN were increased significantly ($p < 0.05$) on day 10. As for day 21, the content of VEGF was increased when compared with that of the model group ($p < 0.05$).

RT-PCR assay

The mRNA levels of related genes in skin assessed by RT-PCR are shown in Figs. 5 and 6. Compared with those of blank control group, the mRNA levels of IL-1 and IL-6 in other groups were significantly upregulated on day 3 and then downregulated on day 10. The mRNA levels of growth factors in YB- and TA-treated groups involving bFGF, TGF-β, HGF, and FN were significantly upregulated on day 3 when compared with the blank control group, especially in the TA (m) group. As for days 10 and 21, there were no significant changes.

Western blotting assay

Based on the results of cytokine and mRNA levels, the Erk 1/2 pathway may be activated by growth factors, thus the Western blot (WB) analyses were performed on Erk 1/2-related proteins. As shown in Fig. 7, the protein levels of bFGF, Erk 1/2, and P-Erk 1/2 were significantly upregulated in YB and TA groups on days 3 and 10 ($p < 0.05$). On day 21, the expression levels of bFGF and P-Erk 1/2 were downregulated in pretreated groups (YB and TA groups), which were near the protein levels in blank control group.

In vitro studies on NIH 3T3 assay

Based on the results shown *in vivo*, we initially investigated the effect on the proliferation of fibroblast NIH 3T3 cells through treatment with different concentrations of TA (0.1–0.4 μg/mL) for 6, 12, and 24 h. The results are shown in Fig. 8, at the 6th hour, the cells grow faster at the concentration of 0.1–0.4 μg/mL TA than the control group ($p < 0.001$). And at the concentration of 0.1 μg/mL TA group, the growth rate increased significantly at the 6th, 12th, 24th hour.

As the results shown in Figs. 9 and 10, the relative mRNA levels of bFGF, HGF, TGF-β, and FN were evaluated, and the levels of bFGF and HGF were increased significantly in the TA groups ($p < 0.001$). The protein concentrations of bFGF and HGF were

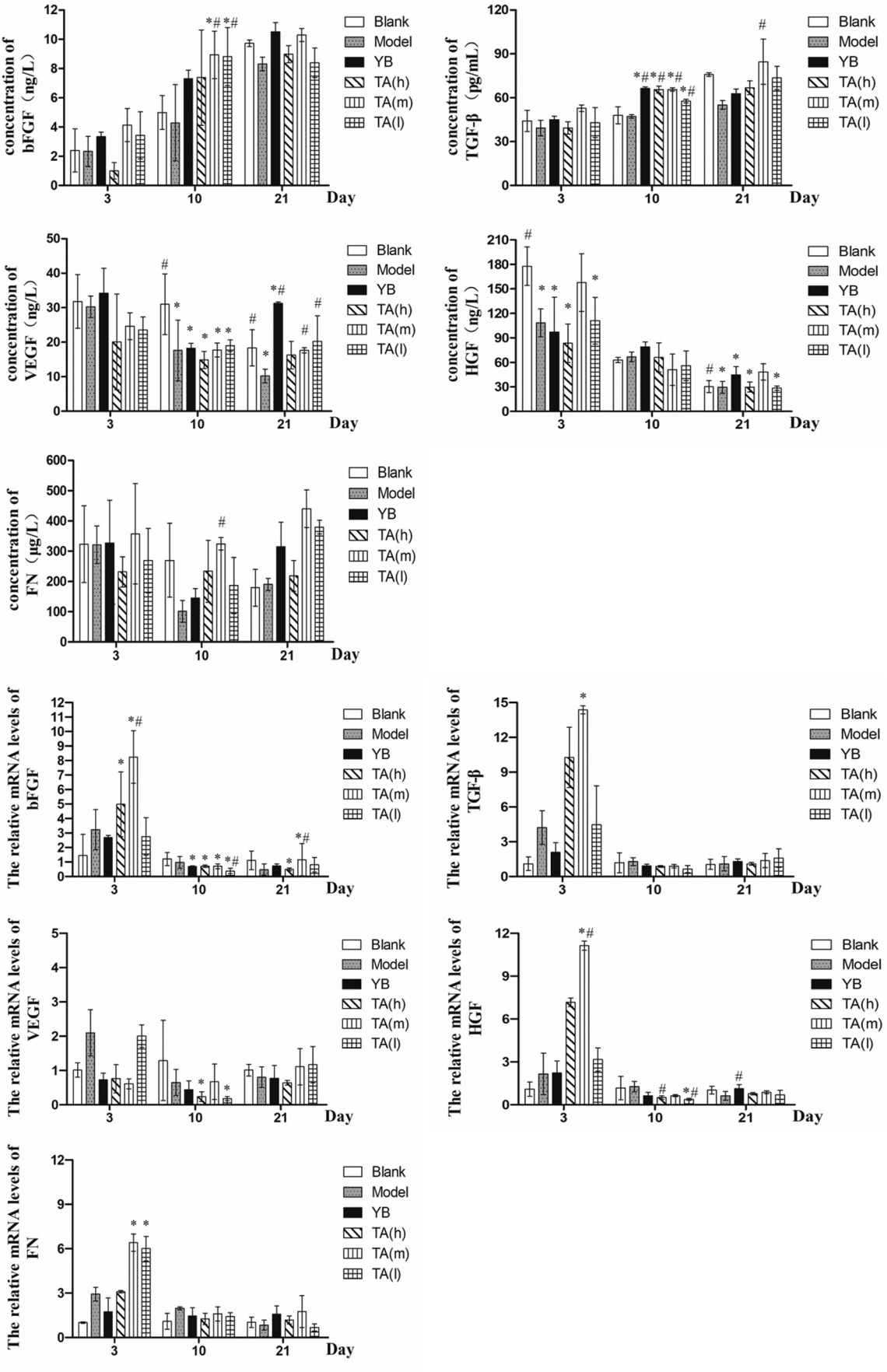

Figure 6. The effects of TA on the content of growth factors were detected by ELISA or RT-PCR. Blank and model represent the groups that were treated as blank control or model group, and YB, TA (h), TA (m), and TA (l) represent the groups that were pretreated with YB, high, middle, and low dose of TA. The values are presented as means ± standard deviation (10 rats per group).*$p < 0.05$ versus blank control group; $^{\#}p < 0.05$ versus model group.

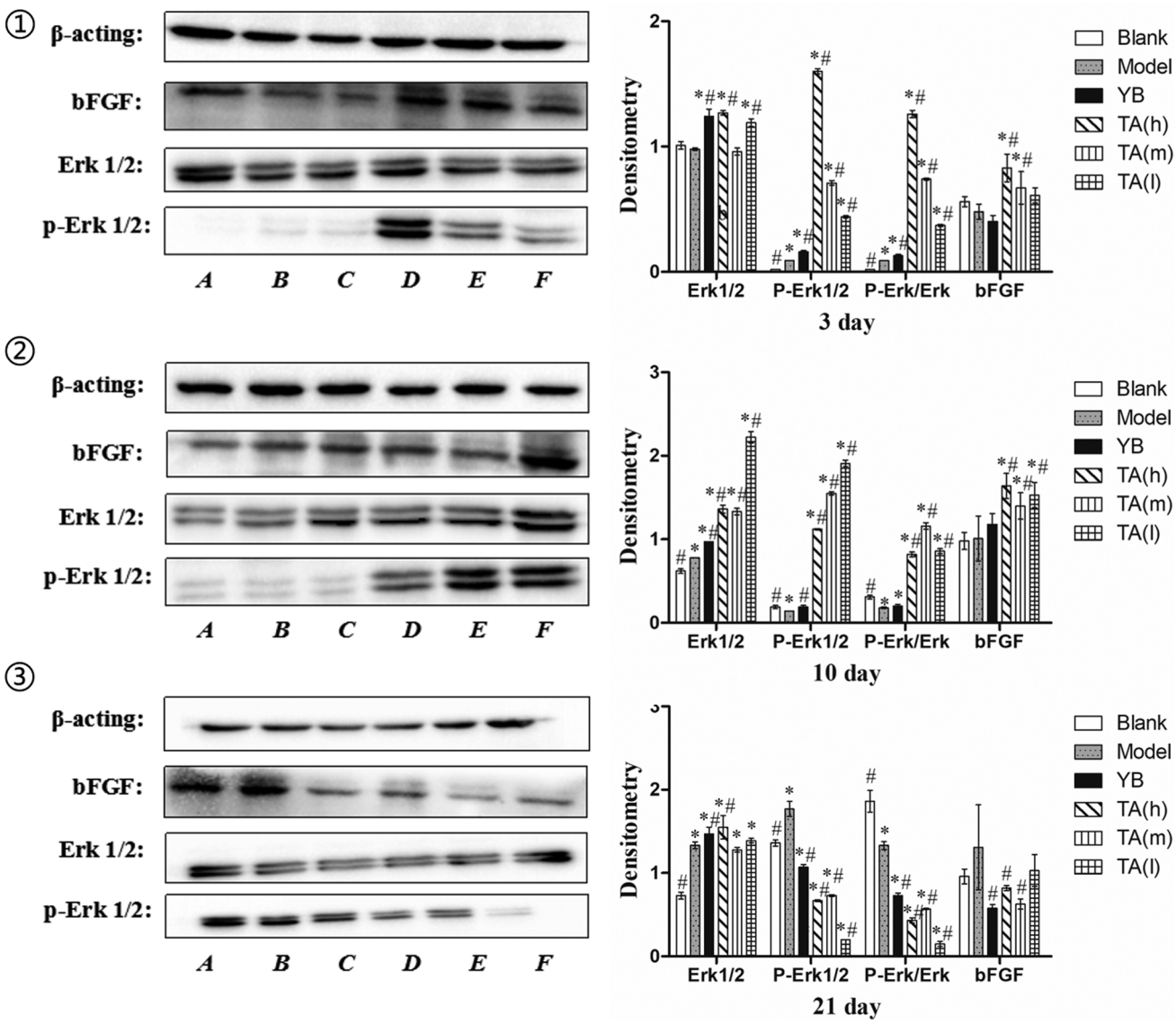

Figure 7. Labels ①, ②, and ③, respectively showed the protein levels of β-actin, bFGF, Erk 1/2, and P-Erk 1/2 in skin, which were assessed by WB on 3rd day, 10th day and 21st day. Blank (A) and model (B) represent the groups that were treated as blank control or model group, and YB (C), TA (h) (D), TA (m) (E), and TA (l) (F) represent the groups that were pretreated with YB, high, middle, and low dose of TA. The values are presented as means ± standard deviation (10 rats per group). $^{*}p<0.05$ versus blank control group; $^{\#}p<0.05$ versus model group. bFGF, basic fibroblast growth factor; WB, Western blot.

evaluated by ELISA, and the expression of bFGF showed significant increase in the 0.1 μg/mL TA group ($p<0.05$). The protein of Erk 1/2 signal pathway was evaluated by WB, and the results showed that the expression of P-Erk 1/2/Erk 1/2 was increased significantly in the 0.1 μg/mL TA group than the control group ($p<0.001$). The protein expression levels of bFGF in all TA groups were increased significantly ($p<0.001$).

DISCUSSION

Wound healing is a dynamic and complex multistep process, the inflammatory cytokines and growth factors play an important role to repair the wound site.[12] To the best of our knowledge, this investigation represents the first study to demonstrate that TA, a natural plant polyphenol astringent, effectively promotes wound healing through the Erk 1/2-mediated signaling pathway.

The wound sizes and histopathology are common ways to evaluate the potency of a vulnerary. Yang *et al.* found that lucidone as a naturally occurring cyclopentenedione could significantly decrease the wound size within 5 days of postwounding.[2] In our research, the wounds were made on rats with sterile dermal biopsy punches and the wound sizes in the YB- and TA-treated rats decreased quickly,

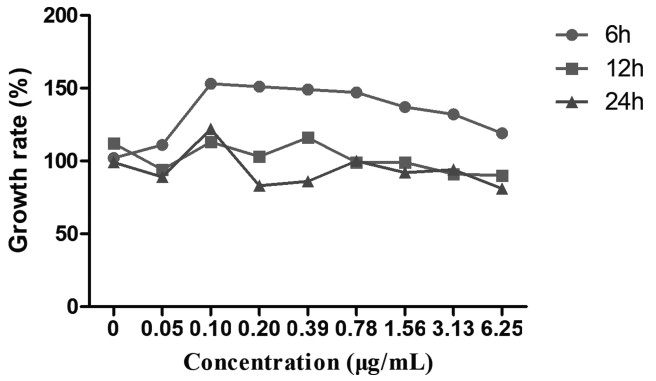

Figure 8. The growth rate of NIH 3T3 cells with different concentrations of TA was assessed by Cell Counting Kit-8. At the concentration of 0.1 μg/mL TA stimulated the increase of the number of cells of NIH 3T3. At the 6th hour, the cells grow faster at the concentration of 0.1–0.4 μg/mL TA than the control group ($p<0.001$). And at the concentration of 0.1 μg/mL TA group, the growth rate increased significantly at the 6th, 12th, and 24th hour. The values are presented as means ± standard deviation.

which got healed >50% in the pretreated rats after 5 days, which was similar with lucidone. The wound closed faster with TA-treatment from 3rd to 9th day, and the rats had formed the scab that could avoid infection and cause slow healing after treatment with high-dose TA for 11 days. In the histopathology study, TA treatment accelerated re-epithelialization and growth of hair follicle. This finding is consistent with Sun *et al*.'s report, in which *Galla Chinensis* solution that contains abundance of TA could improve skin lesions and hair loss in a dose-dependent manner in fungi-infected dogs.[13]

An inflammatory response was caused upon injury to the skin, the epidermal barrier is disrupted, and keratinocytes release prestored inflammatory cytokines including IL-1, IL-6, and IL-10.[3,14] Sun *et al.* had reported that *Galla Chinensis* (1 g/kg) had significant anti-inflammatory activity in the capillary permeability test and carrageenan-induced edema test, and the levels of proinflammatory cytokines were significantly reduced.[15] Our study showed that YB and TA treatment could decrease the contents of IL-1 and IL-6, which were increased by skin lesions. During the inflammatory stage, TA had significant anti-inflammatory activity to protect the body.

Growth factors, cytokines and chemokines, are crucial for coordinating multiple cell types during the healing process, making cutaneous wound healing possible. Proper wound healing is guided by stringent regulation of these agents as well as a wound environment that favors their activity.[3] β-Lapachone promotes wound healing by inducing macrophages to secrete VEGF and EGF for facilitating the growth of other cells.[16] Lin *et al*. showed that mRNA expression levels of the angiogenic cytokines, VEGF, bFGF, and HGF, were all significantly increased in the full-thickness mice, which were treated with Plerixafor (AMD3100) combined with low-dose tacrolimus.[4,17] Our study detected the effects of TA on the content of inflammatory cytokines and growth factors in serum and tissue by ELISA and RT-PCR. The results showed that the levels of growth factors in TA groups were all increased significantly relative to the model group, and the levels of IL-1 and IL-6 were lower, which disclosed that TA could activate the wound site to release growth factors and inhibit the release of inflammatory cytokines. And we also found that the level of HGF was decreased, which was similar to the report that HGF increased

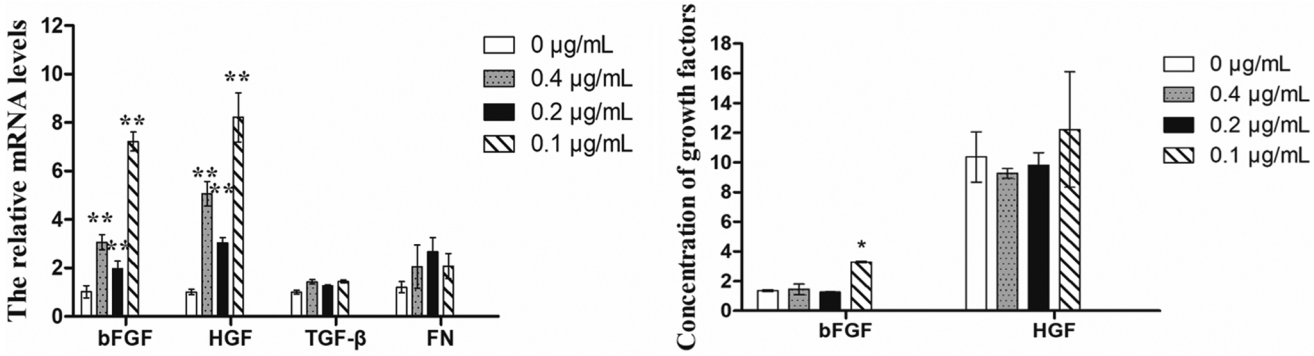

Figure 9. The effects of TA on the content of growth factors were detected by ELISA or RT-PCR. A concentration of 0.1 μg/mL TA stimulated the transcription and secretion of bFGF. The relative mRNA levels of bFGF, HGF, TGF-β, and FN were evaluated, and the levels of bFGF and HGF were increased significantly in TA groups. The protein concentration of bFGF was evaluated by ELISA, which showed significant increase in the 0.1 μg/mL TA group. The values are presented as means ± standard deviation. *$p<0.05$ versus the control group; **$p<0.001$ versus the control group. FN, fibronectin; HGF, hepatocyte growth factor; TGF-β, transforming growth factor-beta.

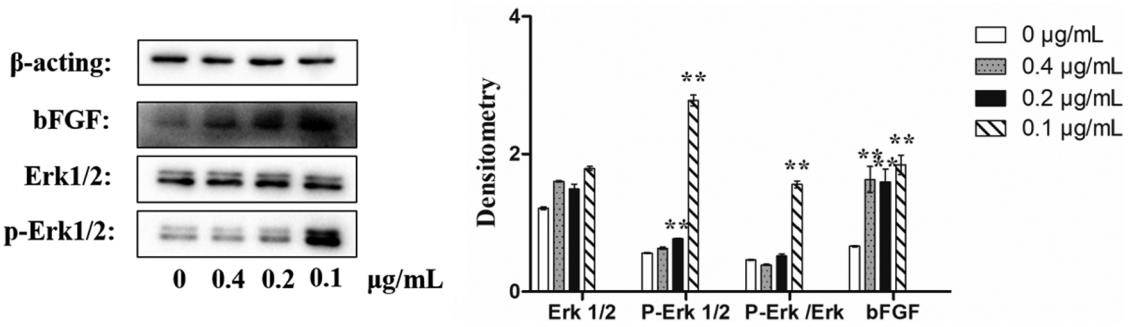

Figure 10. The protein levels of β-actin, bFGF, Erk 1/2, and P-Erk 1/2 in NIH 3T3 were assessed by Western blot. A concentration of 0.1 μg/mL TA activated the Erk 1/2 pathway. The expression levels of P-Erk 1/2/Erk 1/2 were increased significantly in the 0.1 μg/mL TA group than in the control group ($p<0.001$). The protein expression levels of bFGF in all TA groups were increased significantly ($p<0.001$). The values are presented as means $\pm$ standard deviation. $^{**}p<0.001$ versus blank control group.

threefold over the normal level as early as 2 days after wounding, and reached a peak on day 4, then decreased.[18]

When wounded, cell monolayers respond to the disruption of cell–cell contacts by increasing the concentration of growth factors and cytokines at the wound edge, thus initiating proliferation of different cell types, such as keratinocytes and fibroblasts.[19] In this study, we evaluated the effected of TA on NIH 3T3; as the results shown in Figs. 8–10, 0.1 μg/mL TA could increase the cell growth by stimulating the bFGF and activating the Erk 1/2 pathway, which were same as the results shown *in vivo*.

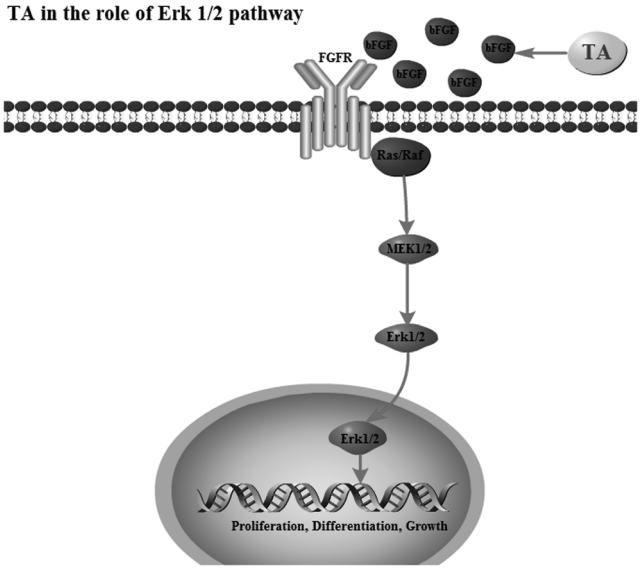

Figure 11. Schematic presentation of TA on skin wound healing molecular mechanism. The mechanism of TA was attributed to activating Erk 1/2 pathway. TA stimulated the growth factors such as bFGF secreted and then bFGF activated Erk 1/2 pathway to make proliferation, differentiation, and growth.

The success of the wound healing process depends on growth factors, cytokines, and chemokines involved in a complex integration of signals that coordinate cellular processes.[3] Mitogen-activated protein kinases (MAPKs) play a central role in mediating intracellular signals from growth factor receptors found at the cell surface to the nucleus.[20–22] Major members of the MAPK family include ERK 1/2, JNK, and p38 MAPK, among which ERK 1/2 plays a key role in mediating proliferation, differentiation, and migration of various cell types.[21,22] The results of ELISA and RT-PCR showed that TA stimulated the body to secrete the growth factors to the injury, but how these factors worked was unknown. This study assessed the endogenous regulation of bFGF and the related intracellular signaling pathway ERK 1/2 in the wound healing response, finding that the protein level of P-Erk 1/2 was increased in the TA group, which means that the Erk 1/2 pathway was activated by TA. In corneal wound healing, both HGF and keratinocyte growth factor have been demonstrated to activate the ERK 1/2 pathway and facilitate wound closure.[16]

TA promotes wound healing for its efficacy in anti-inflammation and secreting growth factors to activate Erk 1/2 pathway on full-thickness rats and promoting the growth of NIH 3T3 (Fig. 11). Taken together, we conclude that TA may be a potential agent for promoting wound healing.

INNOVATION

The wound healing process is divided into sequential, yet overlapping phases: inflammation, proliferation, and remodeling, and the role of TA in wound healing efficacy is unclear, this study, therefore, assesses the effects of TA on wound healing in different periods and the underlying molecular mechanisms.

ACKNOWLEDGMENTS AND FUNDING SOURCES

This research was financially supported by the Sichuan Veterinary Medicine and Drug Innovation Group of China Agricultural Research System (CARS-SVDIP), the Science and Technology Project of Sichuan Province (Grant Nos. 2017NZZJ036, 2018NZ0043, and 2018NZ0064), the Traditional Chinese Medicine Industry Innovation Team of Sichuan Province (Grant No. 2017C015), and the Agricultural Technology Research and Development Project of Chengdu (Grant No. 2015-NY02-00266—NC).

KEY FINDINGS

- In histopathology study, TA treatment accelerated re-epithelialization and growth of hair follicle.
- During the inflammatory stage, TA had significant anti-inflammatory activity to protect the body; TA could activate the wound site to release growth factors during the whole process.
- TA promotes wound healing for its efficacy in anti-inflammation and secreting growth factors to activate Erk 1/2 pathway.
- TA promotes the growth of NIH 3T3 and activates Erk 1/2 pathway on cells.

AUTHOR DISCLOSURE AND GHOSTWRITING

The authors do not have any commercial or financial conflicts of interests to declare. The named authors wrote this article and no ghostwriters were used.

ABOUT THE AUTHORS

Zhongqiong Yin, **PhD**, is a professor in Natural Medicine Research Center, College of Veterinary Medicine, Sichuan Agricultural University, Chengdu. The study was conducted under her guidance. **Yaqin Chen**, **PhD**, is a student in Natural Medicine Research Center, and the main performer of the study. **Xu Song**, **PhD**, is a lecturer in Natural Medicine Research Center. **Lvbo Tian**, **MSc**, **Wenzhi Tong**, **MSc**, and **Fengyu Yang**, **BS**, are students in Natural Medicine Research Center. **Renyong Jia**, **PhD**, is a professor in College of Veterinary Medicine. **Yuanfeng Zou**, **PhD, Lizi Yin, PhD, Lixia Li, PhD, Changliang He, PhD**, and **Xiaoxia Liang**, **PhD**, are professors in Natural Medicine Research Center. **Gang Ye**, **PhD**, and **Cheng Lv**, **MSc**, are lecturers in Natural Medicine Research Center.

REFERENCES

1. Tatara AM, Kontoyiannis DP, Mikos AG. Drug delivery and tissue engineering to promote wound healing in the immunocompromised host: current challenges and future directions. Adv Drug Deliv Rev 2018;129:319–329.
2. Yang HL, Tsai YC, Korivi M, et al. Lucidone promotes the cutaneous wound healing process via activation of the PI3K/AKT, Wnt/β-catenin and NF-κB signaling pathways. BBA Mol Cell Res 2017;1864:151–168.
3. Barrientos S, Stojadinovic O, Golinko MS, et al. Growth factors and cytokines in wound healing. Wound Repair Regen 2008;16:585–601.
4. Lin Q, Wesson RN, Maeda H, et al. Pharmacological mobilization of endogenous stem cells significantly promotes skin regeneration after full-thickness excision: the synergistic activity of AMD3100 and tacrolimus. J Invest Dermatol 2014;134:2458–2468.
5. Ehrlich HP, Hunt TK. Effects of cortisone and vitamin A on wound healing. Ann Surg 1968;167:324.
6. Zen AAH, Nawrot DA, Howarth A, et al. The retinoid agonist tazarotene promotes angiogenesis and wound healing. Mol Ther 2016;24:1745–1759.
7. Sundaram GM, Common JEA, Gopal FE, et al. 'See-saw' expression of microRNA-198 and FSTL1 from a single transcript in wound healing. Nature 2013;495:103.
8. Natarajan V, Krithica N, Madhan B, et al. Preparation and properties of tannic acid cross-linked collagen scaffold and its application in wound healing. J Biomed Mater Res B 2013;101:560–567.
9. Umachigi SP, Jayaveera KN, Kumar CKA, et al. Studies on wound healing properties of Quercus infectoria. Trop J Pharm Res 2008;7:913–919.
10. Su X, Liu X, Wang S, et al. Wound-healing promoting effect of total tannins from Entada phaseoloides (L.) Merr. in rats. Burns 2017;43:830–838.
11. Li K, Diao Y, Zhang H, et al. Tannin extracts from immature fruits of Terminalia chebula Fructus Retz. promote cutaneous wound healing in rats. BMC Complement Altern Med 2011;11:86.
12. Lee SH, Zahoor M, Hwang JK, et al. Valproic acid induces cutaneous wound healing in vivo and enhances keratinocyte motility. PLoS One 2012;7:e48791.
13. Sun K, Song X, Jia RY, et al. In vivo evaluation of Galla Chinensis solution in the topical treatment of dermatophytosis. Evid Based Complement Alternat Med 2017;2017:Article ID 3843595.

14. Werner S, Grose R. Regulation of wound healing by growth factors and cytokines. Physiol Rev 2003; 83:835–870.

15. Sun K, Song X, Jia RY, et al. Evaluation of analgesic and anti-inflammatory activities of water extract of Galla Chinensis in vivo models. Evid Based Complement Alternat Med 2018;2018:Article ID 6784032.

16. Kung HN, Yang MJ, Chang CF, et al. In vitro and in vivo wound healing-promoting activities of β-lapachone. Am J Physiol Cell Physiol 2008;295: C931–C943.

17. Ashcroft GS, Dodsworth J, van Boxtel E, et al. Estrogen accelerates cutaneous wound healing associated with an increase in TGF-β1 levels. Nat Med 1997;3:1209.

18. Yoshida S, Yamaguchi Y, Itami S, et al. Neutralization of hepatocyte growth factor leads to retarded cutaneous wound healing associated with decreased neovascularization and granulation tissue formation. J Invest Dermatol 2003;120: 335–343.

19. Fronza M, Heinzmann B, Hamburger M, et al. Determination of the wound healing effect of Calendula extracts using the scratch assay with 3T3 fibroblasts. J Ethnopharmacol 2009;126:463–467.

20. Yang SL, Han R, Liu Y, et al. Negative pressure wound therapy is associated with up-regulation of bFGF and ERK 1/2 in human diabetic foot wounds. Wound Repair Regen 2014;22:548–554.

21. Keshet Y, Seger R. The MAP kinase signaling cascades: a system of hundreds of components regulates a diverse array of physiological functions. Methods Mol Biol 2010;661:3–38.

22. Cargnello M, Roux PP. Activation and function of the MAPKs and their substrates. The MAPK-activated protein kinases. Microbiol Mol Biol Rev 2011;75:50–83.

Abbreviations and Acronyms

bFGF = basic fibroblast growth factor
ELISA = enzyme-linked immunosorbent assay
ERK = extracellular signal regulated kinase
FGF = fibroblast growth factor
FN = fibronectin
HGF = hepatocyte growth factor
IL-1 = interleukin-1
MAPK = mitogen-activated protein kinases
RT-PCR = real-time polymerase chain reaction
TA = tannic acid
TGF-β = transforming growth factor-beta
VEGF = vascular endothelial growth factor
WB = Western blot
YB = Yunnan Baiyao